Pseudogap term in the magnetic response of cuprate superconductors

R. E. Walstedt, T. E. Mason, G. Aeppli, S. M. Hayden, and H. A. Mook

Phys. Rev. B **84**, 024530 — Published 27 July 2011

DOI: 10.1103/PhysRevB.84.024530

Pseudogap term in the magnetic response of cuprate superconductors

R. E. Walstedt,[1,*] T. E. Mason,[2] G. Aeppli,[3] S. M. Hayden,[4] and H. A. Mook[2]

[1]*Department of Physics, University of Michigan, Ann Arbor, MI 48106*
[2]*Oak Ridge National Laboratory, Oak Ridge, TN 37831*
[3]*London Centre for Nanotechnology and Department of Physics and Astronomy, UCL, London WC1E 6BS, UK*
[4]*H. H. Wills Physics laboratory, University of Bristol, Tyndall Ave.,Bristol, BS8 1TL, UK*

This paper presents a joint analysis of inelastic neutron scattering (INS) and nuclear magnetic resonance (NMR) data on superconducting cuprates, with the aim of a detailed characterization of the dynamical susceptibility $\chi''(\vec{q},\omega)$ at low frequencies and at temperatures ranging from T_c up to room temperature. Using the well-known relation between $1/T_1$ and $\chi''(\vec{q},\omega)$, the analysis shows that the temperature dependence of the nuclear relaxation rate $1/T_1$ is controlled by a combination of dynamic spin-spin correlations between pairs of fluctuating moments in the CuO_2 plane and a time constant proportional to the integral of $\chi''(\vec{q},\omega)$ over the Brillouin zone (BZ). INS data on $\chi''(\vec{q},\omega)$ for $La_{1.86}Sr_{0.14}CuO_4$ (LSCO) and $YBa_2Cu_3O_{6.5}$ (YBCO6.5) are seen to obey ω/T scaling above a transition temperature, then fall to very low values at low temperatures. Thus, there is no evidence in such data for magnetic pseudogap effects, which are known to be quite pronounced in YBCO6.5, but somewhat muted in LSCO. Our analysis of T_1 data shows, however, that above the transition temperature noted above there occurs the onset of another term in $\chi''(\vec{q},\omega)$, which comes to dominate $1/T_1$ at room temperature and above. Analyzed here for the first time, we call this new term "the pseudogap term" $\chi''_P(\vec{q},\omega)$. The onset of $\chi''_P(\vec{q},\omega)$ coincides with the entry into a quantum-critical regime dominated by stripes, but could also be derived from low energy fluctuations resulting from nearby phase transitions characterized by other types of order, such as ring currents. For YBCO6.5 this onset is at $T_c \sim 62K$, but for LSCO, it occurs 20-30K higher than T_c. We model the q-space behavior of $\chi''_P(\vec{q},\omega)$ and discuss its prospects for observation via INS. The occurrence of the foregoing effects is suggested to be widespread among the superconducting cuprates.

PACS numbers: 74.25.nj, 78.70.Nx, 75.40.Gb, 74.72.Kf

I. INTRODUCTION.

Cuprate superconductors are well-known for their unusual normal-state properties. Prominent among these is an extended 'pseudogap' region located above the dome of superconducting transition temperatures T_c (see e.g. a typical phase diagram[1]). Coexistent with the pseudogap phase is a phase with partial magnetic ordering known as "stripes",[2,3] which sets in at $T_{Str} \geq T_c$. Theorists have attempted to connect features in the normal state phase diagram with the phenomenon of high temperature superconductivity itself. There are three main approaches. The first focuses on the disappearance of the Mott-Hubbard antiferromagnet, which is transformed into a resonating valence bond (RVB) state where mobile holes are naturally paired.[4] The second concentrates on 'stripe' correlations as providing the environment needed for superconductivity.[5] The third hypothesizes that the cross-over into the pseudogap region is actually a phase transition to a state with concealed long range order.[6] Experimentally, we have been able to use inelastic neutron scattering (INS) as a function of temperature, composition and magnetic field to map stripe order and fluctuations.[2,7,8] Missing among these probes, however, is a strong magnetic signal having an obvious relation to the by now well-documented pseudogap effects. In the joint NMR and INS analysis presented here we identify a novel low-frequency signal which is correlated with pseudogap formation.

First observed as a gapping out of NMR shift and relaxation parameters,[9–11] the pseudogap has been observed via specific heat[12] as well as with ARPES[13–15] as a genuine charge-energy gap. In more recent ARPES studies, pseudogap excitations known as 'arc fermions' have been characterized in detail.[16,17] Thermally induced changes of the Fermi surface, with concomitant behavior of arc fermion excitations, are clearly related to magnetic manifestations of the pseudogap. However, INS data for $\chi''(\vec{q},\omega)$ show only indirect manifestations of the pseudogap.[18,19] Meanwhile, systems such as $La_{1.86}Sr_{0.14}CuO_4$ (LSCO)[7] and $YBa_2Cu_3O_{6.5}$ (YBCO6.5)[8] yield data for $\chi''(\vec{q},\omega)$ that consist at low frequencies of incommensurate, antiferromagnetically correlated peaks whose intensity exhibits ω/T scaling[20] from T$\sim$ 60K up to room temperature. Pseudogap effects are totally absent from such data. Interestingly, however, nuclear spin-lattice relaxation rates $(1/T_1)$ reported for these systems[21–23] are inconsistent with extrapolation of the INS results to NMR frequencies.

In this paper we present a new, joint analysis of INS and NMR (T_1) data for the systems mentioned above, wherein we propose the existence of a pseudogap fluctuation term $\chi''_P(\vec{q},\omega)$, which has not been identified with INS up to now. Thus, we write $\chi''(\vec{q},\omega) = \chi''_I(\vec{q},\omega)_a + \chi''_P(\vec{q},\omega)$, where $\chi''_I(\vec{q},\omega)_a$ is the INS-measured term with incommensurate peaks along the a axis. Accordingly, we emphasize that locally, $\chi''_I(\vec{q},\omega)_a$ is presumed

to have two-fold symmetry,[8,24] where observed fourfold spectra are thought to arise from domain structure.[7,24–26] The term $\chi''_P(\vec{q},\omega)$ introduced here, which is nonzero once the stripe fluctuations display quantum critical behavior, will be modeled below to interpret the T_1 data. Thus, not only does the strongly evidenced occurrence of such a term clearly explain the hitherto baffling omission of a pseudogap effect from data for $\chi''(\vec{q},\omega)$,[7,8] it also accounts for the disparate behavior of T_1 for the planar ^{63}Cu and ^{17}O nuclear spins in these systems.[22,23] We also show that the thermal and q-space behavior of $\chi''_P(\vec{q},\omega)$ is such that it could have easily been missed up to now by INS experiments on these systems. In sum, the present analysis addresses a major deficiency in our current understanding of the anomalous normal-state physics of cuprates.

II. NUCLEAR RELAXATION WITH DYNAMIC SPIN-SPIN CORRELATIONS.

For the nuclear relaxation analysis we employ the fluctuation-dissipation theorem-based formulation first given by Moriya.[27] Moreover, we further develop the T_1 formulation pioneered for the cuprates by Uldry and Meier,[28] in which explict account is taken of dynamical correlations between fluctuating electronic spins. For the purpose of discussing hyperfine effects, unpaired electronic spins may be regarded as residing on the planar copper sites.[29–31] Referring to the unpaired spin on Cu site j as $\vec{S}_j$, we write the hyperfine (HF) interactions of nuclear spin $\vec{I}_i$ in the form

$$\mathcal{H}_{HF} = \sum_{\alpha,\beta}\sum_{i,j} A_{i\alpha,j\beta} S_{j\beta} I_{i\alpha}, \tag{1}$$

where the sum on j is over Cu sites in the vicinity of $\vec{I}_i$. In the present paper we shall neglect dipolar HF couplings and restrict our attention to HF coefficients of the form $A_{i\alpha,j\alpha} \equiv A_{\alpha ij}$. Following Millis, Monien, and Pines,[31] the relaxation equation is transformed into q-space, giving for spin quantization along the c axis

$$\frac{1}{T_{1c}} = \frac{\gamma^2 k_B T}{4\mu_B^2} \sum_q [A_a(\vec{q})^2 + A_b(\vec{q})^2] \chi''_i(\vec{q},\omega)_a/\omega, \tag{2}$$

where

$$\chi''_i(\vec{q},\omega)_a = (4/g_\alpha^2)\chi''_\alpha(\vec{q},\omega)_a = \frac{4\mu_B^2\omega}{k_B T} S(\vec{q},\omega)_a \tag{3}$$

is a quantity that is isotropic in spin space, and which is closely related to the dissipative susceptibility term $\chi''_\alpha(\vec{q},\omega)_a$ and the dynamic structure factor $S(\vec{q},\omega_0)_a$ as shown.[32] In these equations the subscript a indicates that the two-fold symmetry axis of $S(\vec{q},\omega_0)_a$ in $\vec{q}$-space lies along the a axis. In Eq.(2) the subscripts a,b,c on T_1 and on $A(\vec{q})$ indicate cuprate lattice axes, where in the present paper we shall only be concerned with T_{1c}.

In $\vec{q}$ space a transferred HF coupling from a site located at $\vec{r}_{ij} = (n_a\vec{i} + n_b\vec{j})$ generates a factor $cos(n_a q_a)cos(n_b q_b)$ in the T_1 expression Eq.(2). Such factors are related to the dynamic spin-spin correlation coefficients K_{ij},[28–30] where it is easy to show that

$$K_{ij} = 4\langle \vec{S}_i \cdot \vec{S}_j \rangle = \frac{\int_N d\vec{q}\, cos(n_a q_a a) cos(n_b q_b a) [\chi''(\vec{q},\omega)_a/\omega]_{\omega\to 0}}{\int_N d\vec{q} [\chi''(\vec{q},\omega)_a/\omega]_{\omega\to 0}}, \tag{4}$$

where one sees that $|K_{ij}| \leq 1$. The effective HF couplings which relax the planar ^{63}Cu and ^{17}O nuclei in the cuprate structure involve spin-spin correlations between the first three neighbor pairs, which we write K_{1a}, K_{1b}, K_2, K_{3a}, and K_{3b}. The a,b subscripts denote orientations of $\vec{r}_{ij}$ which lie parallel (a) or perpendicular (b) to the discommensuration (a) axis. For K_2 there is only one coefficient. These correlation coefficients are then given by

$$K_{na,b} = \frac{\int_N d\vec{q}\, g_{na,b}(\vec{q}) [\chi''(\vec{q},\omega)_a/\omega]_{\omega\to 0}}{[\int_N d\vec{q} \chi''(\vec{q},\omega)_a/\omega]_{\omega\to 0}}, \tag{5}$$

n = 1,2,3, where $g_{1a,b} = cos(q_{a,b}a)$; $g_2 = cos(q_a a)cos(q_b a)$; and $g_{3a,b} = cos(2q_{a,b}a)$. For susceptibilities that peak near $\vec{Q} = (\pi,\pi)$, it is clear that $K_{1a,b}$ will be negative, but that K_2 and $K_{3a,b}$ will be positive.

Lastly, we introduce the parameter[28]

$$\tau_{eff}(T) = \frac{k_B T}{\mu_B^2} \int_N d\vec{q} \left[\frac{\chi''(\vec{q},\omega)_a}{\omega}\right]_{\omega\to 0}, \tag{6}$$

proportional to the 'local susceptibility', which acts as a correlation time that includes the particle statistics of the relevant carriers. Uldry and Meier[28] used an iterative fitting procedure to extract values of τ_{eff} from NMR data, but it may also be estimated directly from INS data. Note that data for $\chi''(\vec{q},\omega)_a$ which obey ω/T scaling will lead to a T-independent value for τ_{eff}(T).

Using the foregoing components, the nuclear relaxation rates may then be written

$$\begin{aligned}\frac{1}{^{63}T_{1c}} &= \frac{\gamma_{63}^2}{2}\left[A_{ab}^2 + 4B^2 + 2B^2(4K_2 + K_{3a} + K_{3b})\right. \\ &\left. + 4A_{ab}B(K_{1a} + K_{1b})\right]\tau_{eff}\end{aligned} \tag{7}$$

and

$$\frac{1}{^{17}T_{1c}} = \frac{\gamma_{17}^2}{4}[C_a^2 + C_b^2](2 + K_{1a} + K_{1b})\tau_{eff} \tag{8}$$

for planar ^{63}Cu and ^{17}O, respectively, the two nuclear species of interest. In these equations A_{ab}, B, C_a and C_b are hyperfine tensor components in units of Gauss per unit of spin[22]. These equations are now used to discuss NMR and INS data.

III. JOINT NMR/INS DATA ANALYSES FOR LSCO AND YBCO6.5.

The relaxation equations of the previous section are now employed to conduct a joint analysis of NMR (T_1) data and INS data on the dynamic susceptibility for two cuprates for which extensive, *quantitative* data are available. These were identified in the introduction as LSCO and YBCO6.5. To interpret NMR data we are interested in the low-frequency region of INS data where $\chi''(\vec{q},\omega) \propto \omega$, and for both systems, for temperatures ranging from T_c up to nearly room temperature, one also finds that $\chi''(\vec{q},\omega) \propto 1/T$. Thus, the INS data essentially obey ω/T scaling, a significant feature in terms of early modeling of normal-state cuprate physics.[20] It is also notable that the measured $\chi''(\vec{q},\omega)$ data for these systems consist exclusively of sets of incommensurate peaks surrounding the antiferromagnetic (AFM) point $\vec{Q}$ in q-space. Since evidence has been presented to support the occurrence of dynamical stripes in these systems,[7,8] we invoke the simple physical model developed by Zaanen and co-workers as a way to account for the discommensurations in $\chi''(\vec{q},\omega)$, including the dependence of their splitting on doping level.[25,26]

The observance of ω/T scaling in these systems poses, of course, the problem that such behavior is inconsistent with pseudogap behavior, in which simple magnetic properties "gap out" in the normal state as one approaches T_c.[9–11] Such behavior can only be accounted for by INS fluctuation intensity other than that of the incommensurate peaks which have been studied up to now. As we shall see below, T_1 data give strong evidence for the existence of additional INS intensity which, to our knowledge, has not yet been resolved for the cuprates studied. Here we suggest there to be an additional "pseudogap term" $\chi''_P(\vec{q},\omega)$, so that $\chi''(\vec{q},\omega) = \chi''_I(\vec{q},\omega)_a + \chi''_P(\vec{q},\omega)$. In the analysis below we estimate the amplitude, q-space characteristics, and temperature dependence of the new term $\chi''_P(\vec{q},\omega)$.

A. The case of LSCO.

The incommensurate peak INS spectrum for LSCO has been studied now for many years.[7,33] Our first step is to use the calibrated data given by Aeppli, *et al.*,[7] which we denote $\chi''_I(\vec{q},\omega)_a$, to evaluate the $K_{na,b}$'s (Eq.(5)) and τ_{eff} (Eq.(6)), denoted $K_{Ina,b}$ and τ_{eI}, respectively. Calculations were performed using a two-peak form factor fitted to INS data.[34] Values of $K_{Ina,b}$ so obtained are plotted vs. T in Fig. 1 for $35K \leq T \leq 300K$. It is noteworthy that there are dramatic differences between longitudinal (a) and transverse (b) correlations relative to the discommensurations for the first and third neigbors.

Calculated values of τ_{eI} are plotted vs. T in Fig. 2a (triangles, solid lines). The approximately constant values above $T \sim$ 50K reflect ω/T scaling behavior for $\chi''_I(\vec{q},\omega)_a$. Below 50K, however, the data descend toward zero in a roughly linear fashion. We suggest that $T \sim$ 50K marks the entry into the quantum critical regime associated with stripes in LSCO, giving rise to ω/T scaling above that point.[25,26]

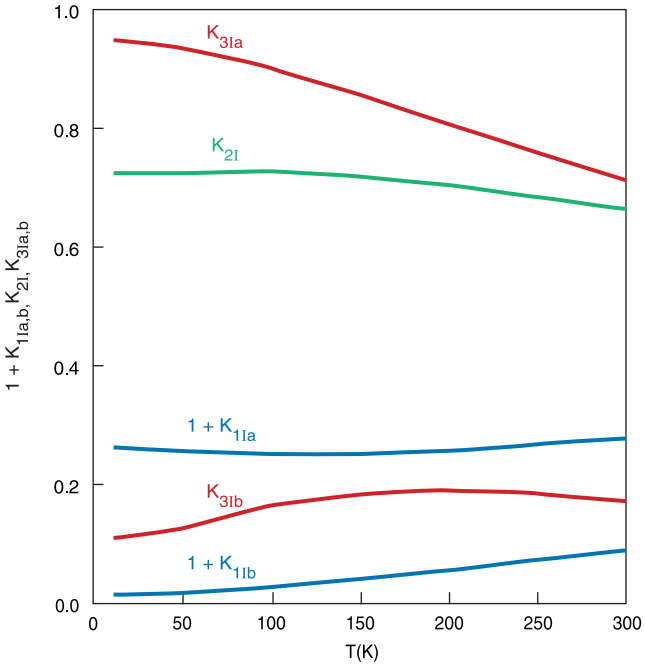

FIG. 1: The spin-spin correlation factors $K_{nIa,b}$ defined in Eq.(5) (with $\chi''(\vec{q},\omega) = \chi''_I(\vec{q},\omega)_a$) are plotted as a function of temperature for LSCO. The coefficients $g_{1a,b}(\vec{q})$ and $g_{3a,b}(\vec{q})$ have twofold symmetry and therefore differ along the (a) axis (K_{1Ia} and K_{3Ia}) and along the (b) axis (K_{1Ib} and K_{3Ib}). Since the $K_{1Ia,b}$'s are negative, they are presented as $1 + K_{1Ia,b}$, which is how they occur in Eq.(8).

We next compare the results for τ_{eI} with estimates of τ_{eff} derived from T_1 data[21,22] using Eq.(7) and (8). To do this, we employ values of the HF constants derived from NMR shift data[35] and values of the $K_{na,b}$'s calculated with Eq.(5), as described above. While there is only a single relaxation rate for ^{63}Cu by symmetry, there are two distinguishable rates for the ^{17}O stemming from the two-fold symmetry of the discommensurations. Since only a single rate was observed,[22] it is presumed either that a flip-flop mechanism is present to maintain a single ^{17}O nuclear spin temperature, or the stripe domain boundaries are fluctuating, so that each site automatically averages the two rates to yield the composite rate given by Eq.(8). Results for τ_{eff} obtained from T_1 data are plotted in Fig. 2a as squares and circles for the ^{63}Cu and ^{17}O nuclear spins, respectively. For comparison, the curve of τ_{eff} vs. T deduced for YBCO7 by Uldry and Meier[28] is shown as a dashed line, reflecting the fact that the T_1 process in LSCO is substantially stronger than that for YBCO7.

In Fig. 2a, the values of τ_{eff} derived from T_1 are seen to agree moderately well with the INS curve (τ_{eI}) for $T \leq$ 50K, considering that there are no adjustable

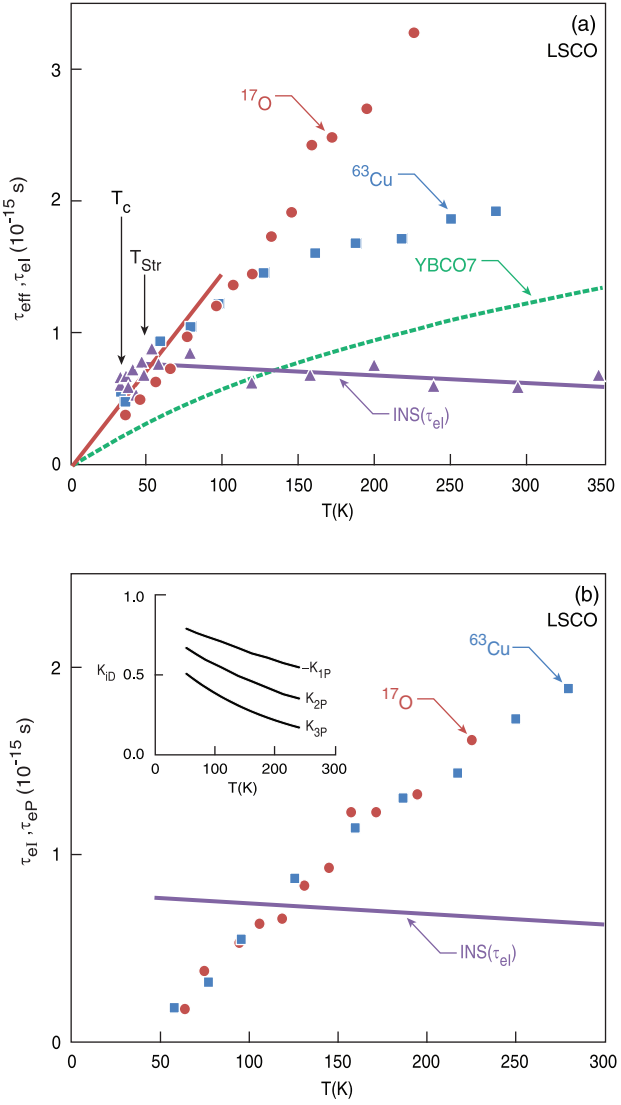

FIG. 2: (a) Values of τ_{eI} and τ_{eff} determined as given in the text for LSCO are plotted vs. T. Values of τ_{eI} (solid triangles) were calculated using $\chi''(\vec{q},\omega) = \chi''_I(\vec{q},\omega)_a$ in Eq.(6). The solid line is a linear regression showing approximate ω/T scaling for $T > T_{Str} \sim 50$K. Values of τ_{eff} obtained from T_1 data with Eq.(7) and (8) are also plotted for ^{63}Cu (squares) and ^{17}O(circles), respectively. The Korringa-like behavior of the τ's below T_{Str} is highlighted by the solid red line. Data for ^{17}O are scaled to that line for the analysis in part (b). For a general comparison, values of $\tau_{eff}(T)$ for YBCO7 obtained by Uldry and Meier[28] for that system are shown as a dashed line. (b) Values of τ_{eP} obtained with Eqs.(9) and (10) using the same T_1 data as above are plotted against temperature. For this purpose, values of the K_{nP}'s derived from a squared-Lorentzian model are used (see text). The K_{nP}'s with their fitted temperature dependence are shown in the inset. The solid line representing the behavior of τ_{eI} from part (a) is replotted here for comparison.

parameters.[36] Above T_{str} they increase rapidly to values much higher than the τ_{eI}. In addition, the ^{63}Cu and ^{17}O-derived values also show substantial disagreement with one another. We interpret these behaviors to mean that T_{str} marks the onset of the pseudogap term $\chi''_P(\vec{q},\omega)$ which then accounts for the great increase of τ_{eff} over τ_{eI}. Further, we conclude that values of $K_{na,b}(T)$ for $\chi''_P(\vec{q},\omega)$ are markedly different from those derived from $\chi''_I(\vec{q},\omega)_a$. With appropriate values for the $K_{na,b}(T)$, the ^{63}Cu and ^{17}O curves for τ_{eff} should coincide.

Our next step is to re-analyze the T_1 data in a way that explicitly takes account of $\chi''_P(\vec{q},\omega)$, which we model in an approximate way. Thus, we have $\chi''(\vec{q},\omega) = \chi''_I(\vec{q},\omega)_a + \chi''_P(\vec{q},\omega)$, leading to two sets of terms in the expressions for $1/T_1$. The resulting forms may be written

$$\frac{1}{^{63}T_{1c}} = \frac{1}{^{63}T_{1Ic}} + \frac{\gamma_{63}^2}{2}\left[A_{ab}^2 + 4B^2(1+2K_{2P}+K_{3P}) + 8A_{ab}BK_{1P}\right]\tau_{eP} \quad (9)$$

and

$$\frac{1}{^{17}T_{1c}} = \frac{1}{^{17}T_{1Ic}} + \frac{\gamma_{17}^2}{2}[C_a^2 + C_b^2]((1+K_{1P})\tau_{eP}, \quad (10)$$

where the T_{1Ic}'s are calculated with Eqs.(7) and (8), respectively, using $\tau_{eff} = \tau_{eI}$, and $K_{nab} = K_{nIab}$. K_{nP} and τ_{eP} are then formally defined using $\chi''_P(\vec{q},\omega)$ in Eqs.(5) and (6), respectively.

Our principal goal here is to use Eqs.(9) and (10) to extract estimates of τ_{eP} from data for both $1/^{17}T_{1c}$ and $1/^{63}T_{1c}$, which we have endeavored to put into agreement with one another. To do that, it is necessary to model $\chi''_P(\vec{q},\omega)$ and make systematic estimates of the K_{nP}. For this purpose we follow Aeppli, *et al.*[7], adopting a squared Lorentzian form of unit amplitude $\chi''_P(\vec{q},\omega)/\chi''_P(peak) = q_w^4/(q_w^2+q_x^2+q_y^2)^2$ with the origin at $\vec{Q} = (\pi,\pi)$. With this symmetric form there are only three correlation coefficients K_{nP}, n=1,2,3 (Eq.(5)), where K_{1P} is substantially negative. Further, since $^{17}T_{1c}$ (Eq.(10)) varies rapidly with K_{1P}, while $^{63}T_{1c}$ (Eq.(10)) is more weakly dependent on K_{nP}, the width parameter q_w may be varied at each temperature to bring τ_{eP} values derived from ^{63}Cu and ^{17}O into coincidence. We adopt this condition as a method for determining the temperature variation of q_w.

Results of this procedure for LSCO are presented in Fig. 2b, with the corresponding values of K_{nP} shown in the inset. The squared Lorentzian model for $\chi''_P(\vec{q},\omega)$ gives a satisfactory account of the data, where we have also taken $K_{1P}(T) = -0.81exp[-(T-50)/600]$ to bring the squares and round dots into reasonable agreement. At room temperature, the $\chi''_P(\vec{q},\omega)$ contributions to the T_1 processes are seen to clearly predominate over $\chi''_I(\vec{q},\omega)_a$. The width parameter for $\chi''_P(\vec{q},\omega)$ varies between $q_w \sim 0.6$ and ~ 1.3 (units of a^{-1}) for $50K < T < 300K$. q_w is therefore similar to the displacement of the incommensurate peaks (~ 0.77) in LSCO. Below we consider the feasibility of resolving $\chi''_P(\vec{q},\omega)$ with INS techniques.

B. The case of YBCO6.5.

While LSCO has only a weak pseudogap, YBCO6.5 has stood from the earliest days as a classic pseudogap

system.[9–11] There now exists for YBCO6.5 a fairly complete, quantitative INS data set, discussed by the authors in terms of dynamical stripe behavior.[8] Low-frequency data for $\chi''_I(\vec{q},\omega)_a$ exhibit clear-cut ω/T scaling, yielding the horizontal solid line in Fig. 3a for τ_{eI}. The INS data show a 70/30 division between the populations of the two possible stripe domains and exhibit a very nearly constant width parameter up to room temperature.[8] The YBCO6.5 data differ from LSCO in that the (INS) values of K_{nI} lead, through Eq.(7) and (8) with measured HF constants[35], to the widely disparate dash-dot curves for τ_{eff} in Fig. 3a. Such a discrepancy in the region below $T_c \sim$ 62K suggests a sharp difference in the peak widths for $\chi''_I(\vec{q},\omega)_a$ between the INS and NMR samples. We remedy this by broadening the $\chi''_I(\vec{q},\omega)_a$ peaks by a factor $\sim$ 2.5 to approximate those for the powdered NMR sample. This leads to unification of the τ_{eff} curves at T $<$ 62K, as shown by the blue square and red circle points in Fig. 3a. Such a surprising broadening effect represents the difference between oriented powder samples used for the T_1 measurements[23] and single crystals used for the INS studies, most likely due to different degrees of chain oxygen ordering. We have calculated $K_{nIa,b}$ (inset, Fig. 3b) using a form factor with discommensurations only along the a axis based on the form given by Stock et al.[8]. The resulting temperature-independent correlation coefficients are $K_{1Ia} = -0.83$; $K_{1Ib} = -0.85$; $K_{2I} = 0.74$; $K_{3Ia} = 0.57$; $K_{3Ib} = 0.61$.

Values of τ_{eff} deduced from T_1 data[23] using Eqs.(7) and (8) agree very nicely with τ_{eI} data (solid line) in Fig. 3a at $T_c \sim$ 62K, again with no adjustable parameters. As with LSCO, the τ_{eff} curves show a sharp increase over τ_{eI} and a strong divergence from one another at T $>$ 62K. To find consistent values of τ_{eP} for YBCO6.5, we again model $\chi''_P(\vec{q},\omega)$ using the squared Lorentzian form as for LSCO. We also use the same exponential form for $K_{1P}(T)$. The resulting convergence of curves for τ_{eP} (squares and circular dots, Fig. 3b) is quite successful. In this case $K_{1P}(T)$ = -0.87$exp[-(T-62)/725]$ decays a bit more slowly and begins with a somewhat narrower peak ($q_w \sim$ 0.44 at T = 62K). The incommensurability $\sim$ 0.38, however, is less than q_w, so that the progressively broadening profile of $\chi''_P(\vec{q},\omega)$ will form something of an elevated baseline for the incommensurate peaks. Such a background will be difficult to detect with unpolarized neutrons.

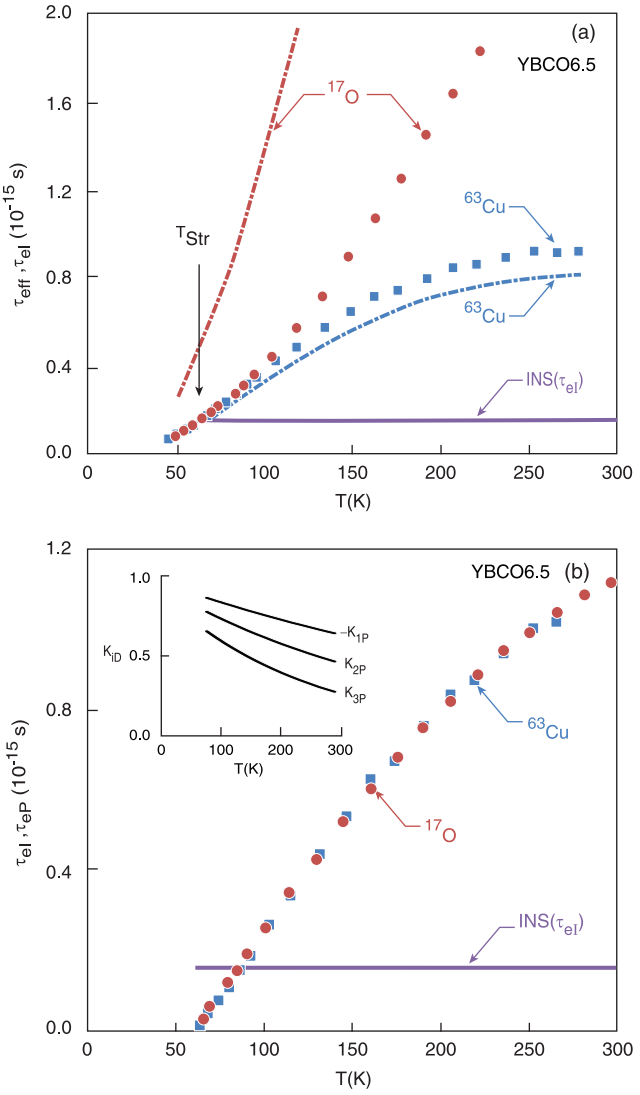

FIG. 3: Plots of τ_{eff}, τ_{eI}, and τ_{eP} are presented for YBCO6.5 similar to the LSCO case in Fig. 2a Values of $\tau_{eI}(T)$ for YBCO6.5, calculated with Eq.(6) using INS data from Ref. 8, are shown as a solid line that obeys ω/T scaling. Values of τ_{eff} obtained with Eq.(7) for the ^{63}Cu and with Eq.(8) for the ^{17}O from T_1 data[23] using values of $K_{nIa,b}$ are plotted as dash-dot lines. The disparity between the dash-dot lines for ^{63}Cu and ^{17}O is attributed to a disparity in incommensurate peak widths between NMR and INS samples and is corrected using adjusted peak widths (see text), leading to the curves showing filled squares (^{63}Cu) and circles (^{17}O). (b) Values of τ_{eP} obtained with Eq.(9) and (10) using T_1 data[23] are plotted against temperature. Calculation of the K_{nP}'s is described in the text. A solid line representing the behavior of τ_{eI} from INS data (see part (a)) is replotted here for comparison. The K_{nP}'s with their fitted temperature dependences are shown in the inset.

IV. DISCUSSION AND CONCLUSIONS

The τ_{eP} curves in Fig. 2b and 3b are qualitatively similar, with τ_{eP} vanishing nearly linearly as T declines toward T_{Str}, while bending over towards room temperature. At the latter point, the new term contributes far more to $1/T_1$ than do the incommensurate peaks. Values of τ_{eI}, which are considerably smaller for YBCO6.5 than for LSCO, obey ω/T scaling and also do not display a spin gap until the materials become bulk superconductors at T_c. The experimental conclusion is therefore clear - the much-celebrated magnetic pseudogaps in these systems are gaps in the new term deduced from T_1 data, which accounts for more spectral weight than the incommensurate spin fluctuations at NMR frequencies. Moreover, given the strong evidence that the stripe (incommensurate) fluctuations which dominate low- and medium energy neutron measurements compete with su-

perconductivity, it is the pseudogap terms that are much more likely to form a pair binding texture.

Some time ago, in the first quantitative test of the magnetic fluctuation-dissipation theorem, a joint analysis of NMR-INS data on LSCO was presented[22]. That work was only a partial success because of its rather simple treatment of the T_1 process. At the time, a two-band model was called for, but there is no longer any clear motivation for such a model[37]. However, NMR shift analyses have been put forth recently giving evidence for a 'two-component' shift structure[38]. We suggest that the two-part structure for nuclear relaxation described in the present work could, via the Kramers-Kronig relation, form the basis in principle for a two-component NMR shift. In practice, there are no $\chi''(\vec{q},\omega)$ data near $\vec{q}=\vec{0}$ to provide a quantitative basis for a shift estimate. However, the proposed NMR shift structure is regarded as a natural extension of the present two-component model for $\chi''(\vec{q},\omega)$. We emphasize that the latter model does not imply two independent bands of charge carriers. Instead, the two terms correspond to fluctuations toward two ordered states, with the incommensurate peaks corresponding to the long-studied stripes, and the second 'pseudogap' term corresponding e.g. to the Varma ring currents.[6] Indeed, what we observe is consistent with the Ising-like scenario for ring current order proposed by Varma and collaborators, where cooling below the 'pseudogap' temperature suppresses the low energy fluctuations to the extent to which the order is established and plaquette reversal is gapped out.

It is useful to examine the prospects for direct observation of the momentum and frequency dependent $\chi''_P(\vec{q},\omega)$ susceptibility term through further INS measurements. The magnitude of τ_{eP} and the spin-spin correlation parameters permit an estimate of the size and shape of $\chi''_P(\vec{q},\omega)$. For LSCO, a squared Lorentzian model for $\chi''_P(\vec{q},\omega)$ based on the latter results would be of similar width to the splitting of the incommensurate peaks in $\chi''_I(\vec{q},\omega)_a$ and $\sim 10\%$ of their height for a scan through adjacent incommensurate peaks at $\mathrm{T} = 100\,\mathrm{K}$. Such a scan is pictured in Fig. 4. The intensity distribution shown is not inconsistent with experimental spectra taken at temperatures $50\mathrm{K} \leq \mathrm{T} \leq 300\mathrm{K}$[7]. It is important to note that the form we have used to model $\chi''_P(\vec{q},\omega)$ was chosen for its simplicity, and that other momentum-dependent terms having broad maxima at other points in the BZ might also account for these data.

This is, of course, the motivation for further neutron experiments. The associated signal would be difficult, but not totally impossible to distinguish from other backgrounds in INS. Such searches, and associated phonon background calculations, should be strongly emboldened by the present work, which is based on an exact theoretical relationship between the spin-fluctuation T_1 process and $\chi''(\vec{q},\omega)$.[27,31] At points where quantitative correspondence is expected (at and below T_{Str} for LSCO and at T_c for YBCO6.5), it is remarkably well confirmed (see Figs. 2a and 3a). Moreover, the joint analysis of ^{17}O and

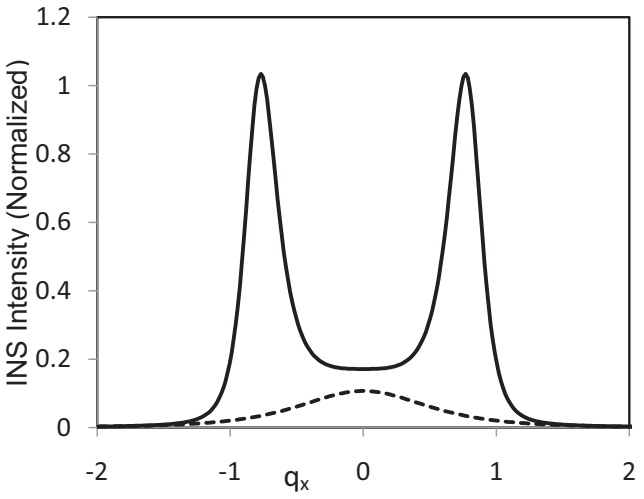

FIG. 4: Normalized profile representing a scan of $\chi''(\vec{q},\omega)$ for LSCO, at low frequencies, through a center point $\mathrm{Q} = (\pi,\pi)$ along the q_x axis, with q_x in units of a^{-1}. The solid line represents $\chi''_I(\vec{q},\omega)_a + \chi''_P(\vec{q},\omega)$ in terms of the fitting functions given in the text [34]. The dashed line shows the squared-Lorentzian profile of $\chi''_P(\vec{q},\omega)$ alone. The parameters used here correspond to peak widths, correlation factors, and relative amplitudes given in Fig.2 for T = 100K.

^{63}Cu T_1 data for YBCO6.5 confirms the work of Uldry and Meier on that system[28], while for LSCO it constitutes the first comprehensive understanding of both T_1 measurements for that compound.

We thank B. S. Shastry and J. Zaanen for highly informative conversations. This manuscript has been authored by UT-Battelle, LLC, under Contract No. DE-AC05-00OR22725 with the U.S. Department of Energy.

* walstedt@umich.edu

[1] S. A. Kivelson, G. Aeppli, and V. Emery, Proc. Nat. Acad. Sci. **98**, 11903 (2001).

[2] J. M. Tranquada, B. J. Sternlieb, J. D. Axe, Y. Nakamura, and S. Uchida, Nature **375**, 561 (1995); J. M. Tranquada, J. D. Axe, N. Ichikawa, A. R. Moodenbaugh, Y. Nakamura, and S. Uchida, Phys. Rev. Lett. **78**, 338 (1997).

[3] C. V. Parker, P. Aynajian, E. H. da Silva Neto, A. Pushp, S. Ono, J. Wen, Z. Xu, G. Gu, and A. Yazdani, Nature **468**, 643 (2010).

[4] P. W. Anderson, P. A. Lee, M. Randeria, T. M. Rice, N. Trivedi, and F. C. Zhang, J. Phys.: Condensed Matter **16**, R755 (2004).

[5] S. A. Kivelson, I. P. Bindloss, E. Fradkin, V. Oganesyan, J. M. Tranquada, A. Kapitulnik, C. Howald, Rev. Mod. Phys. **75**, 1201 (2003).

[6] V. Aji and C. M. Varma, Phys. Rev. B **75**, 224511 (2007)); B. Fauqué, Y. Sidis, V. Hinkov, S. Pailhes, C. T. Lin, X. Chaud, and P. Bourges, Phys. Rev. Lett. **96**, 197001 (2006).

[7] G. Aeppli, T. E. Mason, S. M. Hayden, H. A. Mook, and J. Kulda, Science **278**, 1432 (1997).

[8] C. Stock, W. J. L.. Buyers, R. Liang, D. Peets, Z. Tun, D. Bonn, W. N. Hardy, and R. J. Birgeneau, Phys. Rev. B **69**, 014502 (2004).

[9] W. W. Warren, Jr., R. E. Walstedt, G. F. Brennert, R. J. Cava, R. Tycko, R. F. Bell, and G. Dabbagh, Phys. Rev. Lett. **62**, 1193 (1989).

[10] H. Alloul, T. Ohno, and P. Mendels, Phys. Rev. Lett. **63**, 1700 (1989).

[11] A. Goto, H. Yasuoka, and Y. Ueda, J. Phys. Soc. Japan **65**, 3043 (1996).

[12] J. W. Loram, K. A. Mirza, J. R. Cooper, and W. Y. Liang, Phys. Rev. Lett. **71**, 1740 (1993).

[13] J. M. Harris, Z.-X. Shen, P. J. White, D. S. Marshall, M. C. Schabel, J. N. Eckstein, I Bozovic, Phys. Rev. B **54**, R15665 (1996).

[14] A. G. Loeser, Z.-X. Shen, D. S. Dessau, D. S. Marshall, C. H. Park, P. Fournier, and A. Kapitulnik, Science **273**, 325 (1996).

[15] H. Ding, T. Yokoya, J. C. Campuzano, T. Takahashi, M. Randeria, M. R. Norman, T. Mochiku, K. Kadowaki and J. Giapintzakis, Nature (London) **382**, 51 (1996).

[16] U. Chatterjee, M. Shi, A. Kaminski, A. Kanigel, H. M. Fretwell, K. Terashima, T. Takahashi, S. Rosenkranz, Z. Z. Li, H. Raffy, A. Santander-Syro, K. Kadowaki, M. R. Norman, M. Randeria, and J. C. Campuzano, Phys. Rev. Lett. **96**, 107006 (2006).

[17] A. Kanigel, M. R. Norman, M. Randeria, U. Chatterjee, S. Souma, A. Kaminski, H. M. Fretwell, S. Rosenkranz, M. Shi, T. Sato, T. Takahashi, Z. Z. Li, H. Raffy, K. Kadowaki, D. Hinks, L. Ozyuzer, and J. C. Campuzano, Nature Physics **2**, 447 (2006).

[18] P. C. Dai, H. A. Mook, S. M. Hayden, G. Aeppli, T. G. Perring, R. D. Hunt, and F. Dogan, Science **284**, 1344 (1999).

[19] O. J. Lipscombe, B. Vignolle, T. G. Perring, C. D. Frost, and S. M. Hayden, Phys. Rev. Lett. **102**, 167002 (2009).

[20] C. M. Varma, P. B. Littlewood, S. Schmitt-Rink, E. Abrahams, A. E. Ruckenstein, Phys. Rev. Lett. **63**, 1996 (1989).

[21] T. Imai, C. P. Slichter, K. Yoshimura, and K. Kosuge, Phys. Rev. Lett. **70**, 1002 (1993).

[22] R. E. Walstedt, B. S. Shastry, and S-W. Cheong, Phys. Rev. Lett. **72**, 3610 (1994).

[23] M. Takigawa, A. P. Reyes, P. C. Hammel, J. D. Thompson, R. H. Heffner, Z. Fisk, and K. C. Ott, Phys. Rev. B **43**, 247 (1991).

[24] H. A. Mook, P. Dai, F. Dogan, and R. D. Hunt, Nature **404**, 729 (2000).

[25] J. Zaanen, M. L. Horbach, and W. van Saarloos, Phys. Rev. B **53**, 8671 (1996).

[26] J. Zaanen and W. van Saarloos, Physica C **282-287**, 178 (1997).

[27] T. Moriya, J. Phys. Soc. Japan **18**, 516 (1963).

[28] A. Uldry and P. F. Meier, Phys. Rev. B **72**, 094508 (2005).

[29] F. Mila and T. M. Rice, Physica C **157**, 561 (1989).

[30] B. S. Shastry, Phys. Rev. Lett. **63**, 1288 (1989).

[31] A. J. Millis, H. Monien, and D. Pines, Phys. Rev. B **42**, 167 (1990).

[32] The subscript "i" will be henceforward dropped, but the isotropic from of susceptibility defined in Eq.(3) will be used throughout.

[33] T. R. Thurston, P. M. Gehring, G. Shirane, et al., Phys. Rev. B**46**, 9128 (1992).

[34] Fits to data from $\chi_I''(\vec{q},\omega)_a$ were made with the normalized form function $F(\vec{q},\kappa) = a_0^4\kappa^4/[a_0^2\kappa^2 + S_2(\vec{q})]^2$, where $S_2(\vec{q}) = [(q_a^2 - \pi^2\delta^2)^2 + q_b^4 + 4\pi^2\delta^2 q_b^2]/(4\pi^2\delta^2)$. This two-peak function gives a very similar shape and width as the four-peak function used in Ref.[7]. The width parameter κ varies with temperature as $\kappa^2 = \kappa_0^2 + a_0^{-2}(k_BT/E_T)^2$, where $\kappa_0 = 0.034\AA^{-1}$, a_0 is the lattice constant, and E_T = 47 meV.

[35] The HF constants (A_{ab}, B, C_a, C_b) used are (19, 76, 108, 64) for LSCO [22] and (31, 79, 145, 89) for YBCO6.5 [23], respectively, in units of kG/spin. γ_{17}/π = 577.19 Hz/G; γ_{63}/π = 1128.5 Hz/G.

[36] We suggest error limits of ±30% for INS-derived τ_{eff} values for both LSCO and YBCO6.5.

[37] V. Barzykin, D. Pines, D. Thelen, Phys. Rev. B50, 16052 (1994)

[38] J. Haase, C. P. Slichter, and G. V. M. Williams, cond-mat: 0907.0484.